DNA Repair 8 (2009) 330–335

Contents lists available at ScienceDirect

DNA Repair

journal homepage: www.elsevier.com/locate/dnarepair

A der(8)t(8;11) chromosome in the Karpas-620 myeloma cell line expresses only *Cyclin D1*: Yet both *Cyclin D1* and *MYC* are repositioned in close proximity to the 3′ *IGH* enhancer

Amel Dib[a], Oleg K. Glebov[a], Yaping Shou[b], Robert H. Singer[c], W. Michael Kuehl[a,*]

[a] *Genetics Branch, Center for Cancer Research, National Cancer Institute, National Institutes of Health, 8901 Wisconsin Avenue, Bethesda, MD 20889, USA*
[b] *Oncology Biomarkers and Imaging, Novartis Institutes for BioMedical Research, 220 Massachusetts Avenue, Cambridge, MA 02139, USA*
[c] *Department of Anatomy and Structural Biology, Albert Einstein College of Medicine, Albert Einstein Cancer Center, 1300 Morris Park Avenue, Bronx, NY 10461, USA*

ARTICLE INFO

Article history:
Received 20 September 2008
Received in revised form 3 November 2008
Accepted 5 November 2008
Available online 27 December 2008

Keywords:
Multiple myeloma
Karpas-620
Translocations
Cyclin D1
MYC
IgH enhancer

ABSTRACT

The Karpas-620 human myeloma cell line (HMCL) expresses high levels of *Cyclin D1* (*CCND1*), but has a der(8)t(8;11) and a der(14)t(8;14), and not a conventional t(11;14). Fluorescent in situ hybridization (FISH) and array comparative genomic hybridization (aCGH) studies suggest that der(14)t(11;14) from a primary translocation underwent a secondary translocation with chromosome 8 to generate der(8)t(8;[14];11) and der(14)t(8;[11];14). Both secondary derivatives share extensive identical sequences from chromosomes 8, 11, and 14, including MYC and the 3′ IgH enhancers. Der(14), with *MYC* located ~700 kb telomeric to the 3′ *IGH* enhancer, expresses *MYC*. By contrast, der(8), with both *CCND1* and *MYC* repositioned near a 3′ *IGH* enhancer, expresses *CCND1*, which is telomeric of the enhancer, but not MYC, which is centromeric to the enhancer. The secondary translocation that dysregulated MYC resulted in extensive regions from both donor chromosomes being transmitted to both derivative chromosomes, suggesting a defect in DNA recombination or repair in the myeloma tumor cell.

1. Introduction

Multiple myeloma (MM) includes both primary and secondary *IGH* translocations [1,2]. Primary *IGH* translocations, which are thought to occur when B lymphocytes pass through germinal centers, appear to be mediated mostly by errors in *IGH* switch recombination, with breakpoints occurring within or near *IGH* switch regions; but less often they appear to be mediated by errors in somatic hypermutation, with breakpoints occurring within or near *JH* regions [2,3]. These mostly simple reciprocal translocations involve five recurrent partner chromosomal loci and oncogenes: 11q13 (*Cyclin D1* (*CCND1*)), 15%; 6p21 (*CCND2*), 3%; 4p16 (*MMSET* and *FGFR3*), 15%; 16q23 (*MAF*), 5%; and 20q12 (*MAFB*), 2%. Secondary *IGH* translocations, which can occur during any stage of tumor progression, rarely occur near or within *JH* or *IGH* switch regions, and typically are complex rearrangements or insertions. Genomic rearrangements involving a *MYC* gene (*C-* ≫ *N-* ≫ *L-*), which occur as a very late event during tumor progression, provide the best-studied examples of secondary *IGH* translocations in MM [4,5].

The Karpas-620 human myeloma cell line (HMCL) [6] expresses high levels of *CCND1* RNA (M. Kuehl, unpublished). The triploid karyotype includes unbalanced translocations that involve chromosomes 8, 11, and 14, with two copies each of der(8)t(8;11)(q24;q13), der(14)t(8;14)(q24;q32), and der(14)t(1;14)(q11;q32), plus other marker chromosomes, all of which were present in the original tumor cells [6,7]. By fluorescent in situ hybridization (FISH) analyses, we have shown previously that *MYC* co-localizes with *IGH* sequences on der(14), whereas both *CCND1* and *MYC* co-localize with *IGH* sequences on der(8) [5,8].

Hypothesizing that there might have been a primary t(11;14) translocation, followed by a complex secondary translocation that involved *MYC*, we identified and cloned an 11;14 translocation breakpoint fragment. We then performed FISH and array comparative genomic hybridization (aCGH) mapping studies to elucidate the structures of the rearranged chromosomes that contain *MYC* or *CCND1* sequences. In addition, we determined which chromosomes express *MYC* and *CCND1* RNA.

* Corresponding author at: Genetics Branch, Center for Cancer Research, National Cancer Institute, National Institutes of Health, Bethesda Naval Hospital, 8901 Wisconsin Avenue, Building 8, Room 5101, Bethesda, MD 20889-5101, USA.
Tel.: +1 301 435 5421; fax: +1 301 496 0047.
E-mail address: wmk@helix.nih.gov (W.M. Kuehl).

1568-7864/$ – see front matter © 2008 Elsevier B.V. All rights reserved.
doi:10.1016/j.dnarep.2008.11.010

2. Materials and methods

2.1. Somatic cell hybrids

Karpas-620 cells (10^8) were fused with SP2/0 mouse plasmacytoma cells (5×10^7), and somatic cell hybrids were selected in RPMI 1640 medium supplemented with 10% fetal calf serum, 0.1 mM hypoxanthine, 0.4 μM aminopterin, 16 μM thymidine and 1 μM ouabain [9]. There were 60 positive wells, all of which contained mouse *myc*, including all possible expression patterns for human *MYC* and *CCND1* RNA. Subclones of the hybrids were made by limiting dilution in 24 well macrotiter plates. Somatic cell hybrid clones and subclones that contain the human *MYC* gene were identified by a competitive PCR reaction. A human exon 2 primer (GTCAAGCTTAGACTGCCTCCCGCTTTGTGT) and mouse intron 1 primer (TTGGAAGTACAGCACGCTGAA), together with a human/mouse primer (GTAGTCGAGGTCATAGTTCCTGTT), generated 105 and 184 bp products from the human and mouse genomic DNA, respectively. A competitive RT.PCR assay also was used to determine the expression of human *MYC* RNA. An exon 2 human/mouse primer (CCAGGACTGTATGTGGAGCG), together with exon 3 human (GAGGTTTGCTGTGGCCTCCAG) and mouse (TGTGTGTCCGCCTCTTGTCG) primers, generated 482 and 685 bp products, respectively. An RT.PCR assay specific for human *CCND1* used two oligonucleotides (CTGGCCATGAACTACCTGGA and GTCACACTTGATCACTCTGG) that generated a 483 bp product. The presence of Karpas-620 chromosomes – normal 8 and 11, der(8)t(8;11), and der(14)t(8;14) – in the somatic cell hybrid clones and subclones were determined by FISH analyses.

2.2. RNA FISH

The RNA FISH experiments to determine the sites of *CCND1* RNA expression were done using a previously described protocol [10]. A plasmid containing a 16 kb genomic DNA segment that included the *CCND1* gene was used as a probe [11].

2.3. FISH mapping experiments

Three color FISH analyses were done on metaphase chromosomes from Karpas-620, using previously described procedures [5,8]. The EG3-5 probe includes sequences that are 20–35 kb centromeric to the *Eα2* 3′ *IGH* enhancer [12]. The CH probe, which includes sequences that hybridize with both the *Eα1* and *Eα2* 3′ *IGH* enhancers, and most other probes were described and referenced previously [8]. Details regarding BAC probes used for mapping the *CCND1* and *MYC* loci are available upon request.

2.4. Array comparative genomic hybridization

Agilent Human Genome Microarray Kit 244A (Agilent Technologies, Santa Clara, CA, USA) and Agilent Custom 4x44k arrays were used in array CGH analysis. Agilent 244A array contains 236000 60-mer oligonucleotide probes for coding and non-coding genomic sequences with a median distance between probes 8.9 kb. Custom 44k arrays were designed by selecting 39895 non-overlapping oligonucleotide probes from Agilent High Density CGH and ChIP Database Probes spanning 10 genomic regions of interest with an average distance 195 bp between probes (Design 016569; details are available on request). DNA labeling with Cy5- and Cy3-dUTP and array hybridization were done according to the Agilent "Oligonucleotide Array-Based CGH for Genomic DNA Analysis Protocol" (Version 5.0, Publication Number: G4410-90011 V.5.1, November 2007), starting with 3 μg of AluI- and RsaI-digested Karpas-620 and human male DNA. Arrays were scanned and data were extracted from array images by using Agilent Feature Extraction Software (version 9.0) with default settings. Data were imported into R-2.6.0 language and statistical computing environment [13], and analyzed using snapCGH package [14] of BioConductor-1.9 [15]. Background intensity for each spot was removed from foreground hybridization intensity using "minimum" method; data were transformed to $\log_2$ ratio of Cy5- and Cy3-signals, and normalized within array by subtracting median $\log_2$ ratio. Presumptive rearrangement points were determined with two segmentation algorithms that showed good concordance: Circular Binary Segmentation algorithm (as implemented in DNAcopy package [16,17]) and Heterogeneous Hidden Markov Model (BioHMM [18] available in the aCGH package [19]).

2.5. Other experimental procedures

Additional procedures are specifically referenced in the text, or have been described previously [4,20].

3. Results

3.1. Cloning of an 11;14 translocation breakpoint

A Southern blot assay revealed that Karpas-620 DNA lacks sequences immediately 3′ of *Sμ*, and has only germline *Sα* sequences (not shown) [21]. However, it has two different fragments that contain legitimate *5′Sμ-3′Sγ* switch recombination junctions, 6.5 and 8.5 kb SphI fragments (Fig. 1B). A second Southern blot identified 13 and 16 kb BamHI fragments with a 5′Sμ probe, but only the 16 kb fragment hybridized with 5′σμ or JH probes (Fig. 1C). This suggested that the 13 kb fragment included an illegitimate recombination event that occurred within the 1.6 kb separating the distal ends of the 5′Sμ and 5′σμ probes (Fig. 1A). The 13 and 16 kb BamHI fragments were cloned into lambda DASH, selected, and sequenced. A legitimate Sμ*S*γ1 junction was identified in each case. The 16 kb fragment contained only *IGH* sequences, but the 13 kb fragment contained an 11;14 breakpoint (Fig. 1D, E) that was located 880 bp telomeric (5′) to *Sμ*, 343.2 kb centromeric to *CCND1*, and ∼530 bp telomeric to *MYEOV* (11q13:68818198-68821329, NCBI build 35).

3.2. CCND1 is expressed only from der(8) and MYC is expressed only from der(14)

We identified four copies of *CCND1* in Karpas-620, one each on two copies of der(8)t(8;11) and two copies of der(1)t(1;11)(q32;q13) (Table 1) [8]. RNA FISH analyses showed that *CCND1* RNA is expressed only from the two *CCND1* loci that are associated with *IGH* sequences, i.e., der(8)t(8;11) (Fig. 2). Unfortunately, we were unable to identify *MYC* expression by RNA FISH assays. Instead, we made somatic cell hybrids between Karpas-620 and a mouse plasmacytoma cell line, and then analyzed hybrid subclones in an attempt to correlate specific chromosome content with human *MYC* and *CCND1* RNA expression. As expected from the RNA FISH results, *CCND1* RNA was expressed only by hybrid subclones that contain der(8)t(8;11) (data not shown). There are three kinds of chromosomes in Karpas-620 that contain the *MYC* gene [normal 8; der(8)t(8;11); der(14)t(8;14)], with *MYC* associated with *IGH* sequences in the latter two (Table 1) [7,8]. Hybrids containing only normal human chromosome 8 do not express human *MYC* RNA, a result that is consistent with the hypothesis that *MYC* is not expressed from a normal germline allele in most – if not all – HMCL and mouse plasmacytoma [4,22]. Somewhat surprisingly, however, hybrid subclones that contain only der(8) also do

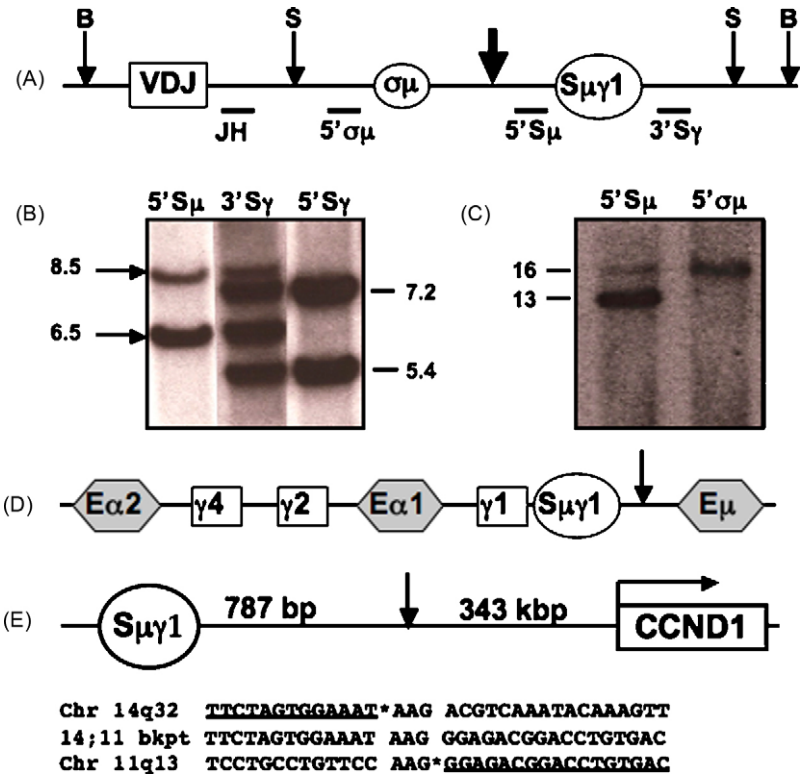

Fig. 1. Identification and sequence of t(11;14) translocation breakpoint in Karpas-620. (A) Map of probes used to detect translocations. Circles and boxes indicate structural elements; thin vertical arrows indicate *Bam HI* (B) and *SphI* (S) restriction sites. Thick vertical arrow indicates site of translocation breakpoint. (B, C) Southern blots of Karpas-620 genomic DNA digested with *SphI* (B) or *BamHI* (C) were hybridized with probes that flank the mu or gamma switch regions, as described previously [21]. The sizes of fragments, in kb, is shown. Arrows in (B) indicate SμSγ legitimate switch recombination fragments. (D, E) the structure of the t(11;14) translocation breakpoint (vertical arrow) is shown, with the telomeric end at the right. The horizontal arrow indicates the direction of transcription of CCND1. The breakpoint includes an overlapping AAG sequence. For Chr 14, the asterisk follows position 105,398,505; and for Chr 11, the asterisk precedes position 68,821,862 (NCBI build 35).

not express human *MYC*, whereas those that contain der(14) do express human *MYC* RNA (Table 2).

3.3. FISH mapping of breakpoints involving the MYC and CCND1 loci in Karpas-620

We did FISH mapping studies to determine the anatomy of rearranged chromosomes that contained sequences from chromosomes 8, 11, and 14. We hoped that this might shed some light on the events that created these rearranged chromosomes, but might also help us understand why *MYC* RNA is not expressed from der(8)t(8;11). Representative results (Table 1) led to the following conclusions. First, both der(8)t(8;11) and der(14)t(8;14) contain sequences from the *MYC*, *CCND1*, and *IGH* loci. Therefore, despite our inability to detect sequences from all three chromosomes using whole chromosome painting probes, these translocations are more correctly designated as der(8)t(8;[14];11) and der(14)t(8;[11];14). Second, there are sizable regions of chromosomes 8, 11, and 14 that are represented on both der(8) and der(14). This indicates that the process that generated these chromosomes was not simple reciprocal rearrangements but included duplication of extensive sequence from each chromosome. Finally, results with probes from the *CCND1* locus suggest that the 11q13 breakpoint in der(11)t(11;13)(q13;q14) shares a simple, reciprocal relationship with the 11q13 breakpoint on der(8) and der(14).

Table 1
FISH mapping rearranged chromosomes in Karpas-620.

A	c-MYC locus	8 wcp	-0.4 Mb	*c-MYC*	+0.4 Mb	+0.55 Mb
	N8 x2	+	+	+	+	+
	der8t(8;14;11) x2	+	+			0
	der14t(8;11;14) x2	+	0			+
B	Cyclin D1 locus	11 wcp	-0.4 Mb	-0.2 Mb	-0.1 Mb	*CCND1*
	der8 t(8;14;11) x2	+	0			+
	der14 t(8;11;14) x2	0	0			0
	der1 t(1;11) x2	+	+	+	+	+
	der11 t(11;13) x2	+	+	0	0	0
C	IgH Locus	14 wcp	-20 kb Eα2	Eα1&2	Cγ	VH
	der8 t(8;14;11) x2	0			+	0
	der14 t(8;11;14) x2	+			+	0
	der14 t(1;14) x2	+	+	+	+	0

FISH mapping results for selected probes are shown. Negative results are light gray and positive but duplicated regions are charcoal.

Table 2
Expression of human MYC RNA in mouse plasmacytoma X Karpas-620 somatic cell hybrid subclones.

Phenotype#	chr 8	der(8)	der(14)	hu MYC
A (2)	+	0	0	0
B (4)	0	+	0	0
C (1)	+	+	0	0
D (2)	+	+	+	+
E (2)	+	0	+	+
F (5)	0	+	+	+

The presence of human chromosomes was determined by FISH analyses. A human specific RT.PCR assay was used to detect human MYC RNA expression in subclones. (#) Phenotype of the hybrid subclones reflects chromosome content, with the number in parentheses reflecting the number of subclones analyzed.

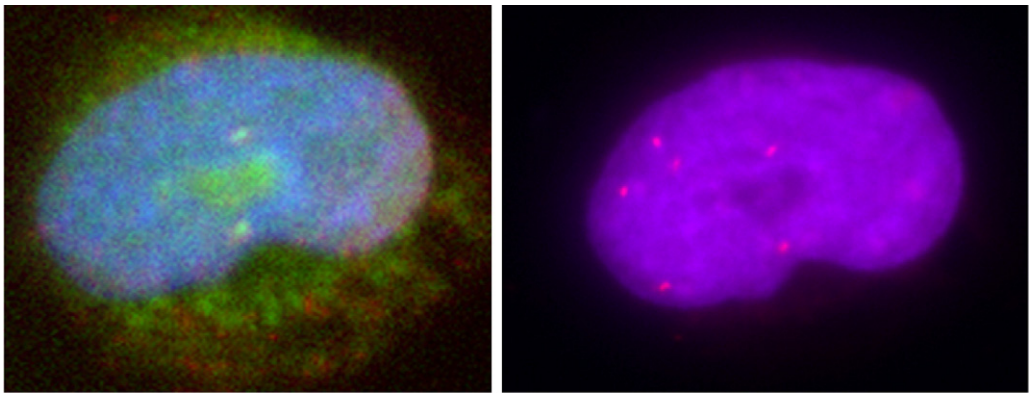

Fig. 2. An RNA FISH analysis shows that CCND1 is expressed only from der(8)t(8;11). The left panel shows an RNA FISH experiment in which a CCND1 probe identifies two sites of CCND1 transcription in a Karpas-620 cell. The right panel shows a DNA FISH experiment on the same cell with a CH probe, demonstrating that the two sites of CCND1 transcription are coincident with two of the six *CH* sequences, both of which are coincident with the *CCND1* gene on der(8)t(8;11) (not shown).

3.4. Mapping of duplicated regions and breakpoints on chromosomes 8, 11, and 14 by array CGH

We used Agilent 244 K and custom arrays to determine the DNA content of the regions on chromosomes 8, 11, and 14 that include the breakpoints and duplicated sequences that are present on der(8)t(8;[14];11) and der(14)t(8;[11];14). Fig. 3A shows that there is a nearly 50% increase in DNA copy number of 828 kb of chromosome 8 sequences, including *MYC* plus sequences 357 kb centromeric and 471 kb telomeric to *MYC*. Fig. 3B shows that there is an approximately 50% increase in DNA copy number of 267 kb of chromosome 11 sequences that start at the cloned 11;14 breakpoint (estimated as 341 kb centromeric to *CCND1* by array CGH, in good agreement with the cloned breakpoint that is 343.2 kb

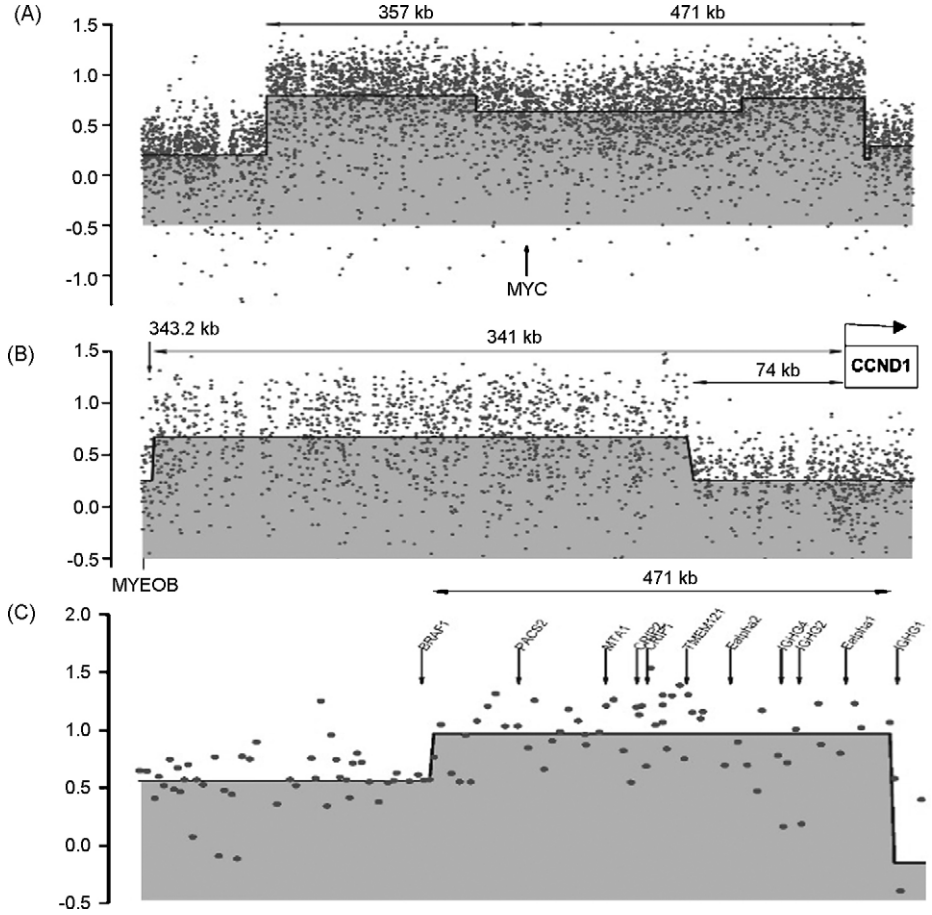

Fig. 3. Array comparative genomic hybridization identifies duplicated sequences and breakpoints. Copy number of Karpas-620 genomic DNA sequences normalized to healthy male DNA was determined by segmental analysis on Agilent custom arrays (A, B), or an Agilent 244K array (C). *MYC* locus (A) results include position of *MYC*, and approximate extent of duplicated sequences centromeric and telomeric to the 5′ end of the *MYC*. *CCND1* locus (B) results include position of *MYEOV* and *CCND1* genes, approximate region of increased copy number, and position of cloned 11;14 breakpoint (vertical arrow) relative to 5′ end of *CCND1* gene. *IGH* locus results (C) include positions of *Eα1&2* 3′ *IGH* enhancers, *IGH* gamma coding regions, five genes centromeric to *Eα2* enhancer, and approximate region of increased DNA copy number. Diagram is not to scale. See text for additional details.

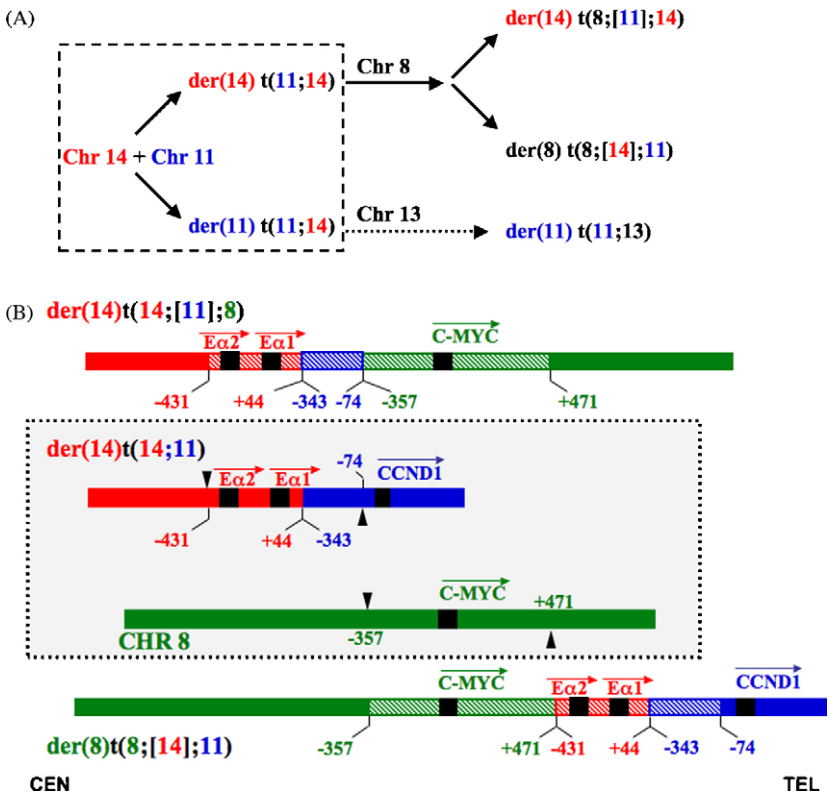

Fig. 4. Primary and secondary translocations that dysregulate *CCND1* and *MYC*. (A) Proposed pathways by which primary and secondary translocations generate der(14)t(8;14), der(8)t(8;11), and der(11)t(11;13) in Karpas-620. (B) Duplicated regions (cross-hatched) and location of breakpoints are shown for der(8)t(8;[14];11) der(14)t(14;[11];8). The reference locations (0) are the centromeric (5′) ends of *MYC* and *CCND1* on chromosomes 8 and 11, respectively; and the telomeric end of the *Eα1* 3′ *IGH* enhancer on chromosome 14. Centromeric and telomeric sites are negative and positive, respectively, with numbers in kb. Boxed chromosomes represent chromosomal precursors and proposed intermediates that are no longer present in the Karpas-620 cell line; arrowheads indicate possible sites of single stranded breaks. The horizontal arrows over the two *Eα* 3′ *IGH* enhancers indicate that their activity may be directed exclusively in a telomeric direction, and the horizontal arrows over MYC and CCND1 indicate their 5′–3′ orientations.

centromeric to *CCND1*), and extend to within 74 kb of *CCND1*. Fig. 3C shows a nearly 33% decrease in copy number of sequences that are ~300 kb centromeric to the *Eα2* 3′ *IGH* enhancer, suggesting that the duplicated region extends about 475 kb centromeric from the cloned 11;14 breakpoint that is located upstream from *Sμ*–*Sγ1*.

4. Discussion

On der(14)t(8;[11];14), *MYC* appears to be located about 670 kb telomeric to the *Eα1* 3′ *IGH* enhancer, which is well within the distance over which this enhancer can act in plasma cell tumors [2]. On der(8)t(8;[14];11), the *CCND1* appears to be located nearly 400 kb telomeric to the *Eα1* enhancer, whereas the *MYC* is located about 770 kb centromeric to the *Eα2* enhancer. The lack of expression of *MYC* on der(8) might be explained by the possible occurrence of insulator sequences immediately centromeric to the *Eα2* 3′ *IGH* enhancer (E. Max, personal communication). However, a more likely explanation is that there are five genes (*HOLE*, *CRIP1*, *CRIP2*, *MTA1*, and *PACS2*) located between the *Eα2* 3′ *IGH* enhancer and the centromeric chromosome 14 breakpoint that is located about 470 kb from *MYC* (Fig. 4B). In any case, this is an example in which juxtaposition of an oncogene close to *IG* enhancer sequences is not associated with dysregulation of the oncogene.

As depicted in Fig. 4A, the structures of der(8)t(8;[14];11)(q24;q32;q13), der(14)t(8;[11];14)(q24;q13;q32), and t(11;13)(q13;q14), as determined by a combination of FISH mapping and array CGH, suggests that a primary t(11;14) translocation was followed by secondary translocations on both derivatives. The secondary translocation that converted der(11)t(11;14) to der(11)t(11;13) appears to be a simple albeit unbalanced translocation, lacking der(13). In contrast, the other secondary translocation converted der(14)t(11;14) to der(8)t(8;[14];11) and der(14)t(8;[11];14) by a process that included duplication of extensive sequences on chromosomes 8 (828 kb), 11 (267 kb), and 14 (475 kb) (Fig. 4B). One possible explanation is duplication of the donor chromosomes (e.g., G2), with double strand breaks at different sites in each of the four chromosomes, followed by heterologous joining of four ends and loss of the other four ends. Another possibility is that there were widely separated single strand breaks on both strands of der(14)t(11;14) and of chromosome 8 (arrowheads in Fig. 4B), followed by a repair process that duplicated extensive sequences at the two breakpoint ends of each chromosome, and then joining of heterologous ends. A third possibility is the involvement of a break-induced replication (BIR) mechanism, although it is difficult to envisage precisely how this might have happened [23,24]. It is thought that B cell specific DNA modification mechanisms (VDJ recombination, somatic hypermutation, and IgH switch recombination) are inactive in normal and tumor plasma cells [2,3]. Therefore, secondary MYC translocations, which occur as late progression events in myeloma tumors, are thought to be mediated by the poorly characterized mechanisms responsible for unbalanced translocations in most kinds of tumors. Even though the mechanism(s) responsible for this unusual secondary translocation are not clear, the occurrence of extensive regions of duplication transmitted from both donor chromosomes to both derivative chromosomes suggests the occurrence of a defect in DNA recombination or repair [25] in the myeloma tumor cell that gave rise to the Karpas-620 cell line.

Conflict of interest statement

The authors declare that there are no conflicts of interest.

Acknowledgements

This research was supported by the Intramural Research Program of the NIH, National Cancer Institute, Center for Cancer Research; and NIH grants CA83208 and EB2060 (R.H.S.). The authors would like to acknowledge Leslie Brents for technical contributions, Ana Gabrea for help in preparation of the manuscript, and also Keith Caldecott, James Haber, and Richard Kolodner for helpful discussions.

References

[1] W.J. Chng, O. Glebov, P.L. Bergsagel, W.M. Kuehl, Genetic events in the pathogenesis of multiple myeloma, Best Pract. Res. Clin. Haematol. 20 (4) (2007) 571–596.
[2] A. Gabrea, P. Leif Bergsagel, W. Michael Kuehl, Distinguishing primary and secondary translocations in multiple myeloma, DNA Repair (Amst) 5 (9–10) (2006) 1225–1233.
[3] P.L. Bergsagel, W.M. Kuehl, Chromosomal translocations in multiple myeloma, Oncogene 20 (2001) 5611–5622.
[4] A. Dib, A. Gabrea, O. Glebov, P.L. Bergsagel, W.M. Kuehl, Characterization of MYC translocations in multiple myeloma cell lines, J. Natl. Cancer Inst. Monograph 39 (2008) 25–31.
[5] Y. Shou, M.L. Martelli, A. Gabrea, et al., Diverse karyotypic abnormalities of the c-myc locus associated with c-myc dysregulation and tumor progression in multiple myeloma, Proc. Natl. Acad. Sci. U. S. A. 97 (1) (2000) 228–233.
[6] E. Nacheva, P.E. Fischer, P.D. Sherrington, et al., A new human plasma cell line, Karpas 620, with translocations involving chromosomes 1, 11 and 14, Br. J. Haematol. 74 (1) (1990) 70–76.
[7] G. Tonon, A. Roschke, K. Stover, Y. Shou, W.M. Kuehl, I.R. Kirsch, Spectral karyotyping combined with locus-specific FISH simultaneously defines genes and chromosomes involved in chromosomal translocations, Genes Chromosomes Cancer 27 (4) (2000) 418–423.
[8] A. Gabrea, M.L. Martelli, Y. Qi, et al., Secondary genomic rearrangements involving immunoglobulin or MYC loci show similar prevalences in hyperdiploid and nonhyperdiploid myeloma tumors, Genes Chromosomes Cancer 47 (7) (2008) 573–590.
[9] R.D. Lane, R.S. Crissman, M.F. Lachman, Comparison of polyethylene glycols as fusogens for producing lymphocyte-myeloma hybrids, J. Immunol. Methods 72 (1) (1984) 71–76.
[10] A.M. Femino, F.S. Fay, K. Fogarty, R.H. Singer, Visualization of single RNA transcripts in situ, Science 280 (5363) (1998) 585–590.
[11] T. Motokura, A. Arnold, Cyclin D and oncogenesis, Curr. Opin. Genet. Dev. 3 (1) (1993) 5–10.
[12] F.C. Mills, N. Harindranath, M. Mitchell, E.E. Max, Enhancer complexes located downstream of both human immunoglobulin Calpha genes, J. Exp. Med. 186 (6) (1997) 845–858.
[13] R. Ihaka, R.R. Gentleman, A language for data analysis and graphics, J. Comput. Graph. Stat. 5 (3) (1996) 299–314.
[14] M.L. Smith, J.C. Marioni, T.J. Hardcastle, N.P. Thorne, snapCGH: Segmentation Normalization and Processing of aCGH Data. Users Guide, Bioconductor, 2006.
[15] R.R. Gentleman, V. Carey, W. Huber, R. Irizarry, S. Dudoit, Bioinformatics and Computational Biology Solutions Using R and Bioconductor, Springer, NY, 2005.
[16] A.B. Olshen, E.S. Venkatraman, R. Lucito, M. Wigler, Circular binary segmentation for the analysis of array-based DNA copy number data, Biostatistics 5 (4) (2004) 557–572.
[17] E.S. Venkatraman, A.B. Olshen, A faster circular binary segmentation algorithm for the analysis of array CGH data, Bioinformatics 23 (6) (2007) 657–663.
[18] J.C. Marioni, N.P. Thorne, S. Tavare, BioHMM: a heterogeneous hidden Markov model for segmenting array CGH data, Bioinformatics 22 (9) (2006) 1144–1146.
[19] J. Frydland, P. Dimitrov, Bioconducor's aCGH Package. User's Guide, Bioconductor, 2007.
[20] A. Dib, T.R. Peterson, L. Raducha-Grace, et al., Paradoxical expression of INK4c in proliferative multiple myeloma tumors: bi-allelic deletion vs increased expression, Cell Div. 1 (2006) 23.
[21] P.L. Bergsagel, M.C. Chesi, E. Nardini, L.A. Brents, S.L. Kirby, W.M. Kuehl, Promiscuous translocations into immunoglobulin heavy chain switch regions in multiple myeloma, Proc. Natl. Acad. Sci. 93 (24) (1996) 13931–13936.
[22] M. Potter, Neoplastic development in plasma cells, Immunol. Rev. 194 (2003) 177–195.
[23] J.E. Haber, Transpositions and translocations induced by site-specific double-strand breaks in budding yeast, DNA Repair (Amst) 5 (9–10) (2006) 998–1009.
[24] B. Llorente, C.E. Smith, L.S. Symington, Break-induced replication: what is it and what is it for? Cell Cycle 7 (7) (2008) 859–864.
[25] J.Y. Hwang, S. Smith, A. Ceschia, J. Torres-Rosell, L. Aragon, K. Myung, Smc5-Smc6 complex suppresses gross chromosomal rearrangements mediated by break-induced replications, DNA Repair (Amst) 7 (9) (2008) 1426–1436.